

Supplementary Information: Strain localization and yielding dynamics in disordered collagen networks

Swarnadeep Bakshi, Vaisakh VM, Ritwick Sarkar, and Sayantan Majumdar

I. MOVIE DESCRIPTIONS

Movie1: In this movie, we show the in-situ deformation of the sample surface in flow-gradient plane correlating with stress vs strain response of collagen network (2 mg/ml) seeded with 1% (v/v) PS. The applied strain ramp rate is 1%/s. The images are captured using a digital camera (Lumenera) fitted with a 5X, long working distance objective (Mitutoyo) at a frame rate of 1 Hz with a resolution of 1200 X 1800 (pixel)². The images are then cropped and compressed such that the spatial resolution is $\sim 1.4 \mu\text{m}/\text{pixel}$. The movie is sped up 14 times as compared to the real time. As mentioned in the main text, we see that network slippage with one of the shearing plates (here, top plate) appears well before the peak stress/breaking stress is reached. The onset of such slippage correlates well with the yield strain of the network (as indicated in the movie). Beyond the peak stress, the detachment (characterized by an elastic retraction of the whole network) takes place from the top plate. The drop in scattered intensity near the top plate close to the yield strain indicates network rarefaction (also see Fig. S8 and the main text) before detachment.

Movie2: In this movie, we show the in-situ deformation of collagen network (2 mg/ml) seeded with 1% (v/v) PS for an applied strain ramp rate of 10%/s. The movie is sped up 1.4 times as compared to the real time. Here also, we find similar correlation of the boundary dynamics with the yield and breaking strains of the network (data not shown). Interestingly, as opposed to Movie1, the network detachment happens from both the plates in this case. Also, we see a clear signature of network rarefaction (drop in scattered intensity) near the shearing boundaries close to yielding (also see Fig. S8). Beyond the network breakage/rupture from both the plates, a clear signature of network contraction away from the plates is seen.

II. TABLE OF PARAMETERS

Parameters obtained from the 8-chain model fitting for three different collagen concentrations.

$\phi = 1\text{mg/ml}$

Temperature ($^{\circ}\text{C}$)	$nk_B T (\text{Jm}^{-3})$	$\frac{L_p}{2L_c}$	$\frac{\xi}{L_c}$
20	80	0.421	0.760
25	180	0.400	0.738
30	200	0.235	0.488
35	270	0.234	0.479
37	380	0.229	0.470

$\phi = 2\text{mg/ml}$

Temperature ($^{\circ}\text{C}$)	$nk_B T (\text{Jm}^{-3})$	$\frac{L_p}{2L_c}$	$\frac{\xi}{L_c}$
20	100	0.390	0.750
25	335	0.366	0.717
28	350	0.306	0.646
30	370	0.284	0.606
35	470	0.252	0.554

$\phi = 3\text{mg/ml}$

Temperature ($^{\circ}\text{C}$)	$nk_B T (\text{Jm}^{-3})$	$\frac{L_p}{2L_c}$	$\frac{\xi}{L_c}$
20	300	0.463	0.790
25	350	0.308	0.658
28	380	0.273	0.607
30	420	0.255	0.579
35	500	0.253	0.574

III. SUPPLEMENTARY FIGURES

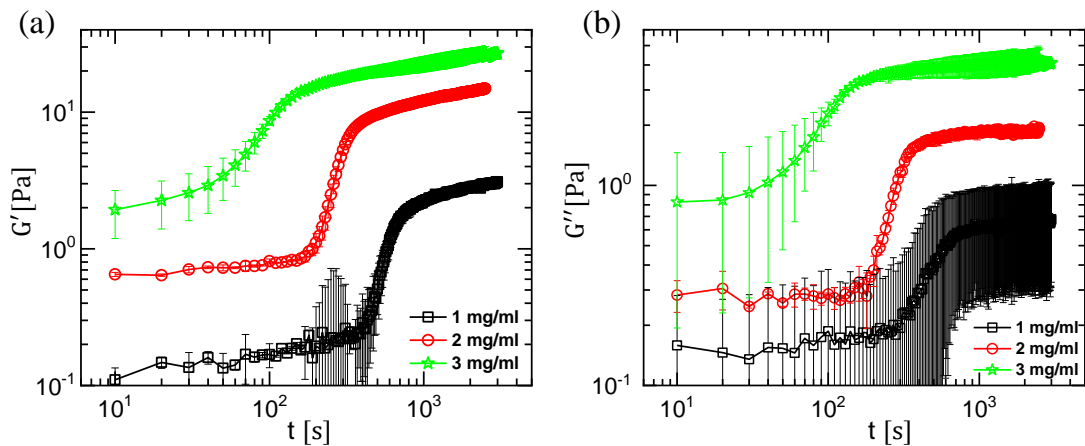


Figure S1: Variation of storage (G' , panel (a)) and loss (G'' , panel (b)) moduli as a function of time during the polymerization of collagen networks. The applied oscillatory strain amplitude is 2% and frequency is 0.5 Hz. As indicated, different symbols represent different concentrations of collagen. The plateau reached after the jump in G' or G'' values represents the polymerized state of the network. The error bars are the standard deviations of two independent measurements under the same condition. Here, polymerization temperature (T) is 25°C in all cases.

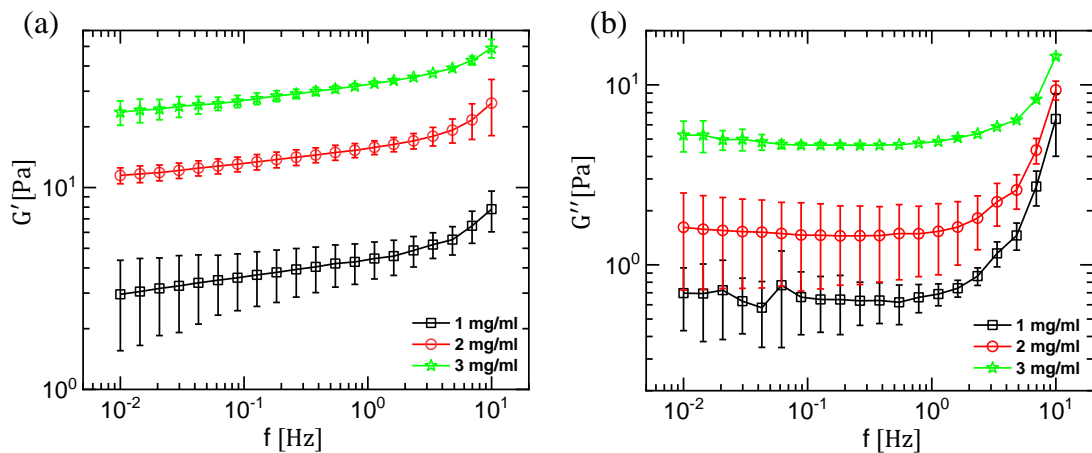


Figure S2: Frequency dependent storage (G' , panel (a)) and loss (G'' , panel (b)) moduli for polymerized collagen networks. The applied oscillatory strain amplitude is 2%. Different symbols represent different concentrations of collagen. $T = 25^\circ\text{C}$. The error bars are the standard deviations of two independent measurements under the same condition. We see that, $G' \gg G''$ over the entire range of frequencies probed.

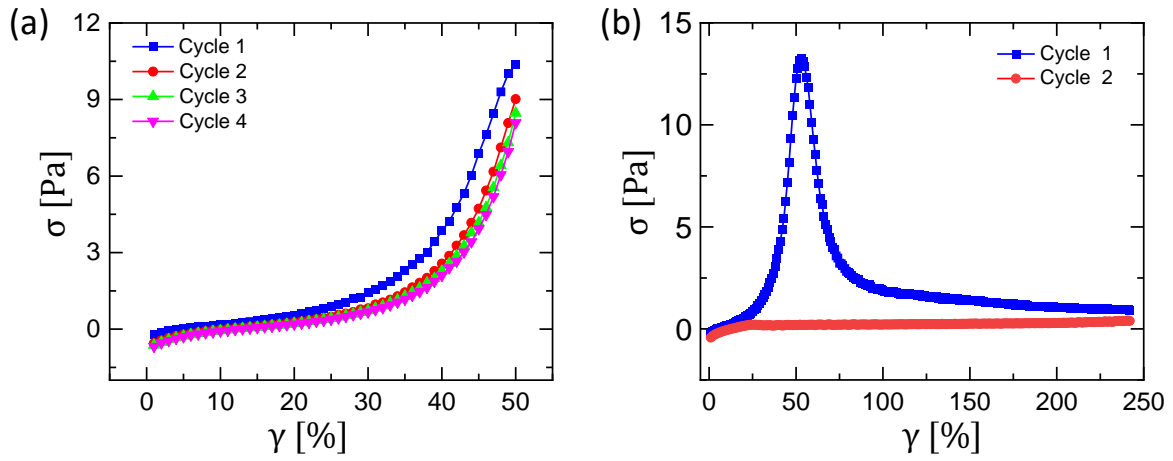


Figure S3: Stress (σ) vs strain (γ) response under repeated deformations for maximum strain below the yield strain (panel (a)) and well beyond yield/breaking strain (panel (b)). Below yield strain ($\gamma < \gamma_y$) the mechanical response is reversible, but above yielding due to breakage of contact with the shearing plates, the response becomes very weak and irreversible. Here, $\phi = 2$ mg/ml and $T = 25^\circ\text{C}$.

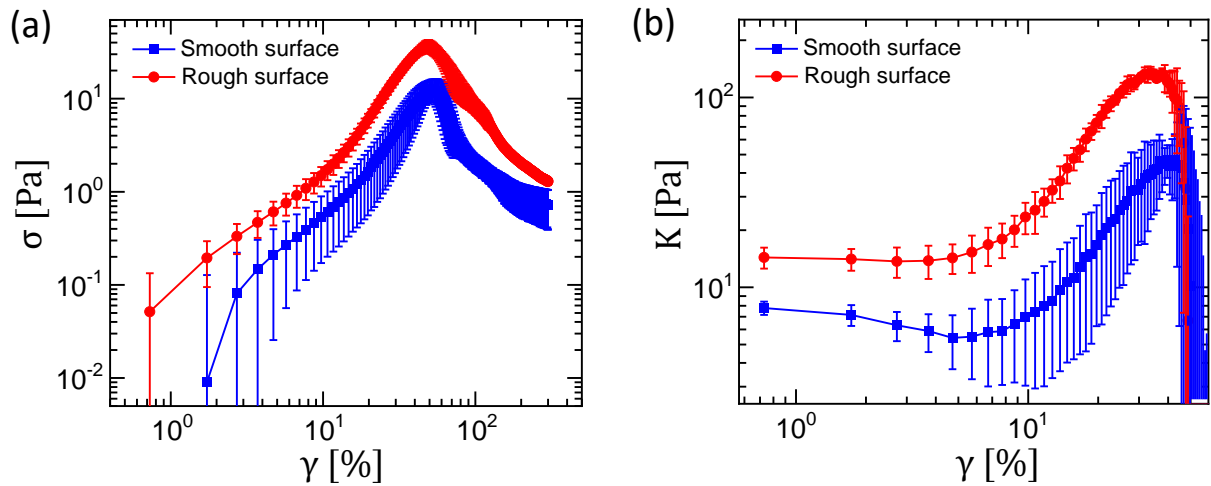


Figure S4: (a) Stress (σ) vs strain (γ) behaviour obtained from cone-plate geometries with smooth and rough (sand-blasted) surfaces as indicated. (b) Corresponding shear-moduli (K) vs γ . The standard deviations of four independent runs under the same condition are shown as error bars. Although, the rheological responses show similar trend, the absolute values of K remain significantly lower for smooth geometry. Here, $\phi = 2$ mg/ml and $T = 25^\circ\text{C}$.

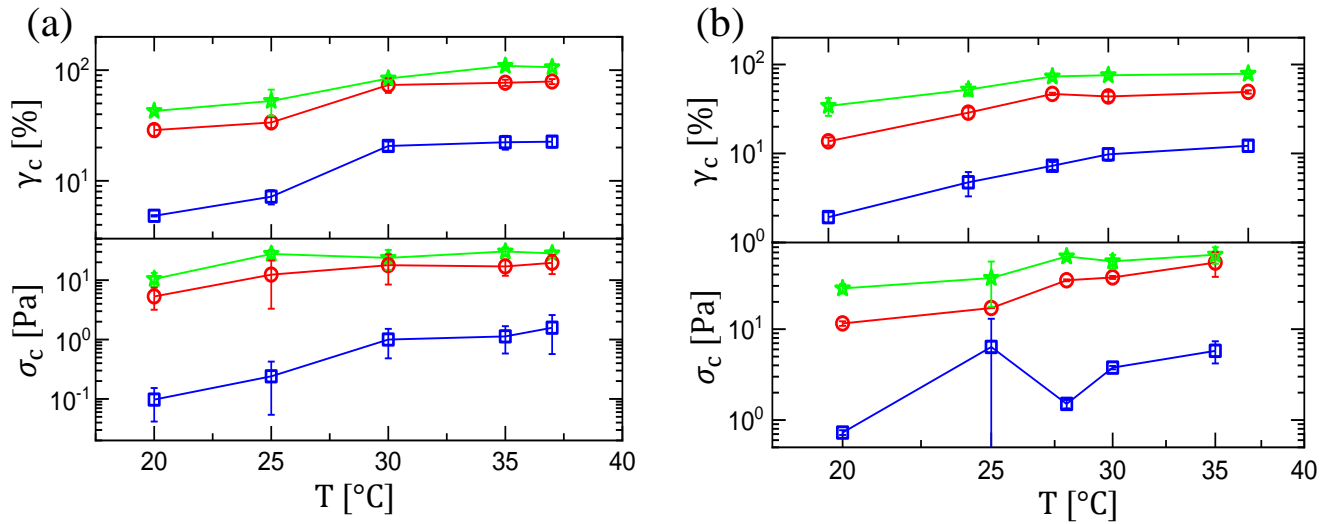


Figure S5: Variation of critical stress and strain values with polymerization temperature for collagen networks. Collagen concentration, $\phi = 1$ mg/ml (panel (a)) and $\phi = 3$ mg/ml (panel (b)). Here, squares represent onset strain/stress, circles represent yield strain/stress and stars represent breaking strain/stress. The error bars are the standard deviations of two independent measurements under the same condition.

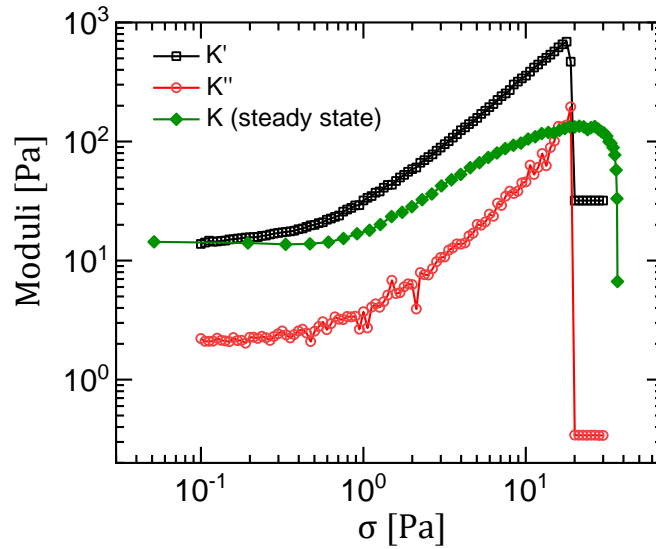


Figure S6: Storage (K') and (K'') components of tangent shear modulus as a function of pre-stress (σ). K' and K'' are obtained from superposing a small sinusoidal stress component (amplitude: 0.1 Pa and frequency: 1 Hz) on the D.C. pre-stress. Also, we compare these with the values of shear moduli (K) under steady state measurement under controlled strain condition (but plotted as a function of stress). We observe that there is a drop in K' , K'' and K values after a strain stiffening response signifying yielding/network-rupture. Here, $\phi = 2$ mg/ml and $T = 25^\circ\text{C}$.

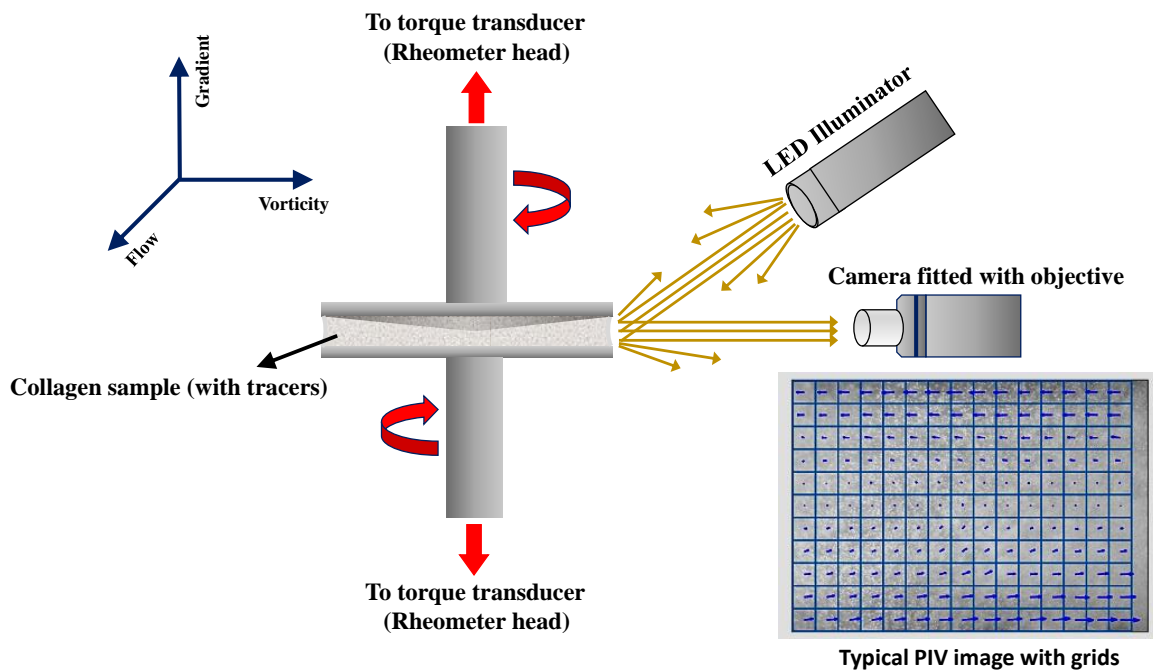


Figure S7: Schematic of the experimental set-up for rheology and in-situ optical imaging. A typical boundary image with superposed grids for PIV analysis is also shown.

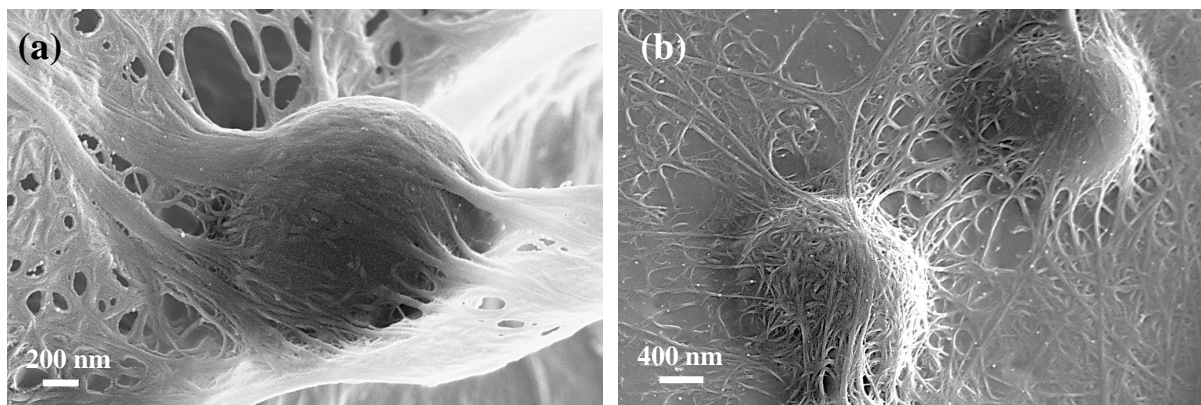


Figure S8: Freeze fracture SEM image of collagen network ($\phi = 2$ mg/ml) seeded with 1% PS of mean diameter of $2.8 \mu\text{m}$. The collagen fibrils seem to have some affinity to stick to the PS surface.

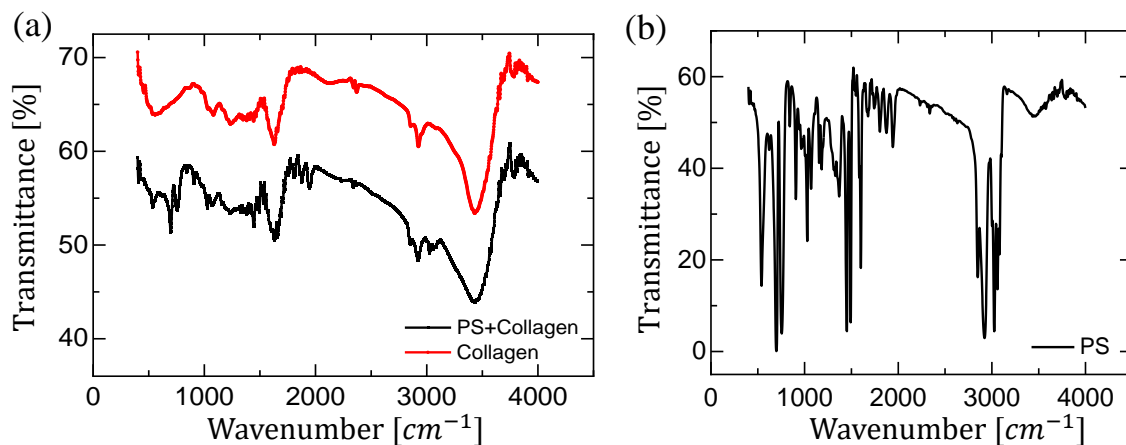


Figure S9: FTIR spectra of pure collagen (shown by the red line in (a)) and collagen mixed with 1% PS (shown by the black line in (a)). FTIR spectrum for only PS particles are shown in (b). As indicated in (a), troughs shown in both the spectra (pure collagen and collagen + PS) are very similar. This indicates that there are no chemical bonding interactions between collagen and PS.

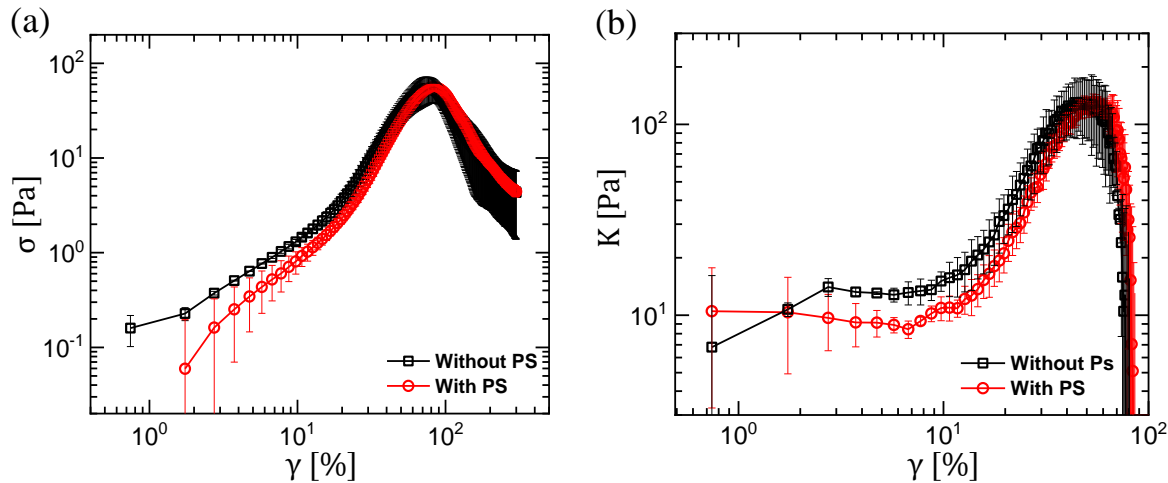


Figure S10: Comparison of network response with and without added PS (1%). We see that stress (σ , panel (a)) and differential shear modulus (K , panel (b)) show very similar behaviour with applied strain (γ) for both the cases. The error bars are the standard deviations of two independent measurements under the same condition. Here, $\phi = 2$ mg/ml and $T = 30^\circ C$.

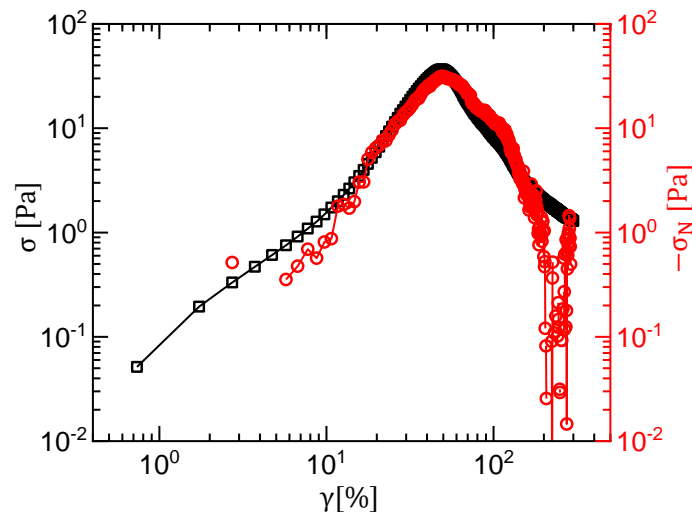


Figure S11: Typical variation of shear stress (σ , shown by the black squares) and negative normal stress (σ_N , shown by the red circles) as a function of applied strain γ for collagen network with $\phi = 2$ mg/ml and $T = 25^\circ\text{C}$. We see that significant negative normal stress (comparable to the shear stress) develops in the network in the strain stiffening regime and reaches a maximum near the yielding.

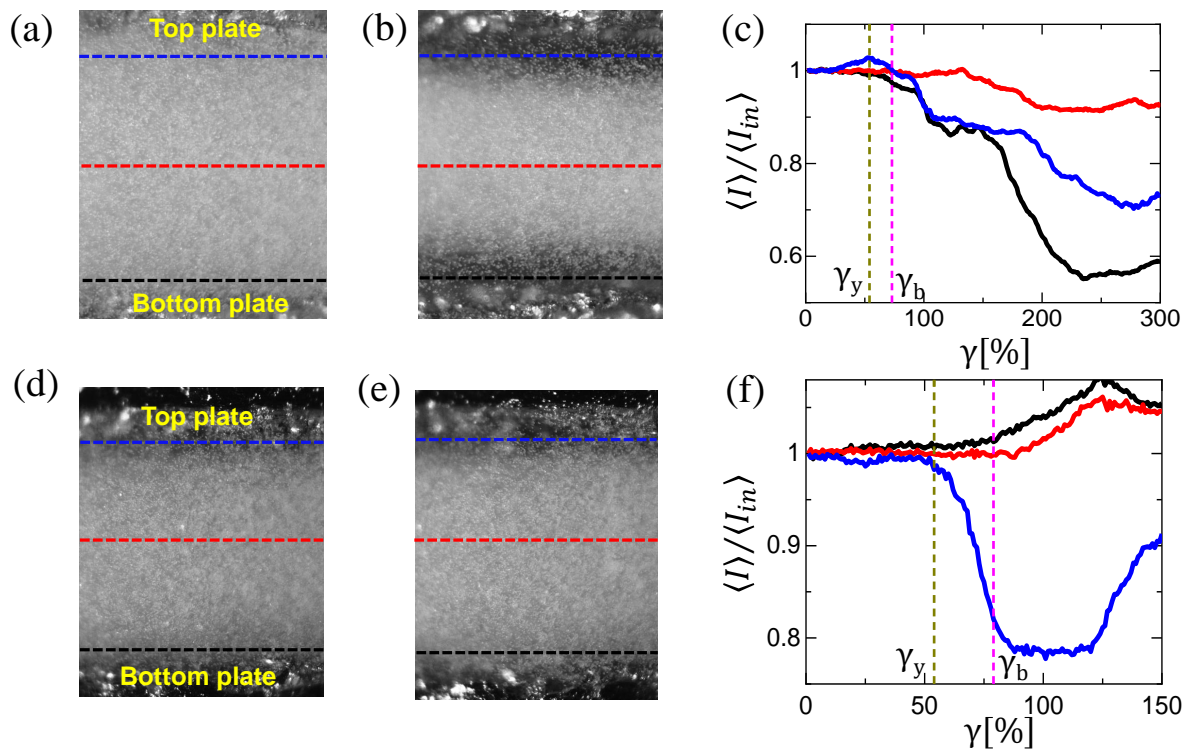


Figure S12: Panels (a), (b), (d) and (e) show typical boundary images of the sample with dashed horizontal lines parallel to the plates indicating the positions where the average intensity (normalized by the initial intensity) as a function of applied strain (γ) are calculated as shown in (c) and (f). Positions near the top and bottom plates indicated by blue and black lines, respectively. Red line indicates a position near the midway between the plates. (a), (b), (c) correspond to a strain ramp rate of 10%/s and (d), (e), (f) correspond to 1%/s. For both ramp rates, the intensity near both the plates (c) or, one of the plates (f) drops significantly beyond the yield (γ_y) and the breaking (γ_b) strains as indicated. Panels (a) and (d) correspond to the initial unstrained state ($\gamma = 0$) of the sample, whereas, (b) and (e) represent that after the network rupture. The drop in scattered intensity near yielding indicates network rarefaction leading to detachment. Here, $\phi = 2$ mg/ml and $T = 30^\circ\text{C}$.

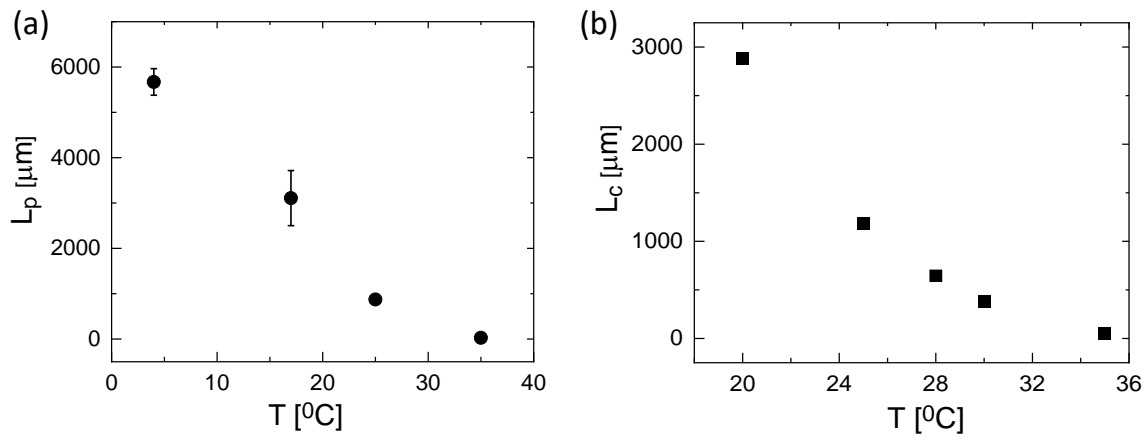


Figure S13: (a) Average persistence length (L_p) estimated from the mean bundle diameters obtained from freeze-fracture SEM data (Fig. 1c, main text) as a function of polymerization temperature. The error bars are the standard deviations obtained from the diameter distributions (Fig. 1c, main text). (b) L_c values (described in the main text) obtained from the 8-chain model using the data for L_p obtained from panel (a). We use the interpolated (cubic-spline) values of L_p for estimating L_c values at the temperatures shown in panel (b). Here, $\phi = 1$ mg/ml.